PHYS 6260 Project Progress Report: Finite Differencing Simulation of Myocardial Tissue

Casey Lee-Trimble

April 2, 2024

Current version of the BidomainSolver:
`https://github.com/ctrimble6/6260_Project_CLT`

1 Cardiac Tissue Simulation

1.1 Field of Study

Studies of the heart at the scale of contractile tissue have advanced rapidly in the last 50 years with the simultaneous advent of two critical technologies. One is the development of fluorescent ion indicators and potentiometric dyes that allow experiments to directly measure electrophysiological parameters with exceptional spatiotemporal resolution[1]. The other is the implementation of increasingly large parallel computational capabilities to solve large systems of differential equations at high speeds, allowing researchers to develop detailed, anatomically scaled models of cardiac cells and tissue.

At the same time, developments in protein-scale studies have produced models of the individual contributions of ion channels and membrane mechanisms that have informed the dynamics of models at the tissue level[2]. As a result, it is becoming more feasible to develop detailed, quantitative models of cardiac tissue which can be validated by currently employed experimental techniques.

1.2 Research Question

The development of models of defibrillation and anti-arrhythmia therapies relies on accurate modeling of the underlying electrophysiology governing the propagation of action potentials, and in particular modeling the response of tissue to external voltages. One of the key mechanisms responsible for the success of defibrillation by external electric shocks is the formation of *virtual electrodes* within the bulk tissue. It is widely hypothesized that spatial heterogeneity in the conductance of the cardiac tissue gives rise to local maxima in the membrane potential that develops in response to an external shock voltage[3][4]. The goal of this project is to simulate a model of cardiac cells using a finite differencing approach, and to

observe the effects of spatially heterogeneous conductivity on the solution for the membrane potential.

2 State of Work

At present, I have written a working Crank-Nicolson solver for the heat diffusion equation, which I will extend to solve the full reaction-diffusion equation in the bidomain model. The key modules that are fully functional at this point are:

- `initialize_v`: initializes the scalar field to be evolved
- `cn_init_1d`: initializes the matrices derived using the Crank-Nicolson method
- `thomas_method`: uses the Thomas algorithm to solve a tridiagonal matrix equation
- `cn_solve`: evolves the scalar field using Crank-Nicolson, utilizing the above methods

2.1 Crank-Nicolson Method

The Crank-Nicolson (CN) method estimates the new value of the potential at a point i by averaging the estimate of the spatial derivative at time t and the future time $t + dt$. If we neglect the external potential and ion current terms in the reaction-diffusion equation of the bidomain model (Eqn 4 in the proposal document), we are left with the heat equation,

$$\frac{\partial V_m}{\partial t} = D\frac{\partial^2 V_m}{\partial x^2}. \tag{1}$$

The CN method casts the diffusion term into finite difference form and averages its solution at two time steps,

$$V_i^{l+1} = V_i^l + \frac{Ddt}{2dx^2}\left[\left(V_{i+1}^{l+1} + V_{i-1}^{l+1} - 2V_i^{l+1}\right)_{future} + \left(V_{i+1}^{l} + V_{i-1}^{l} - 2V_i^{l}\right)_{current}\right] \tag{2}$$

where i is the index of the current grid point and l is the index of the current time step. Representing the constant prefactor as α, we can move all of the values at $t = l + 1$ to the left-hand side, such that

$$-\alpha V_{i+1}^{l+1} + (1 + 2\alpha)\, V_i^{l+1} - \alpha V_{i-1}^{l+1} = \alpha V_{i+1}^{l} + (1 - 2\alpha)\, V_i^{l} + \alpha V_{i-1}^{l} \tag{3}$$

Rewriting this as a matrix equation,

$$\mathbf{A}\vec{V}^{l+1} = \mathbf{B}\vec{V}^{l} \tag{4}$$

where $\mathbf{A}$ and $\mathbf{B}$ are tridiagonal matrices and $\vec{V}$ is vector containing the potential at each point i. Except for the first and last elements, which depend on the boundary condition, $\mathbf{A}$ has (1+

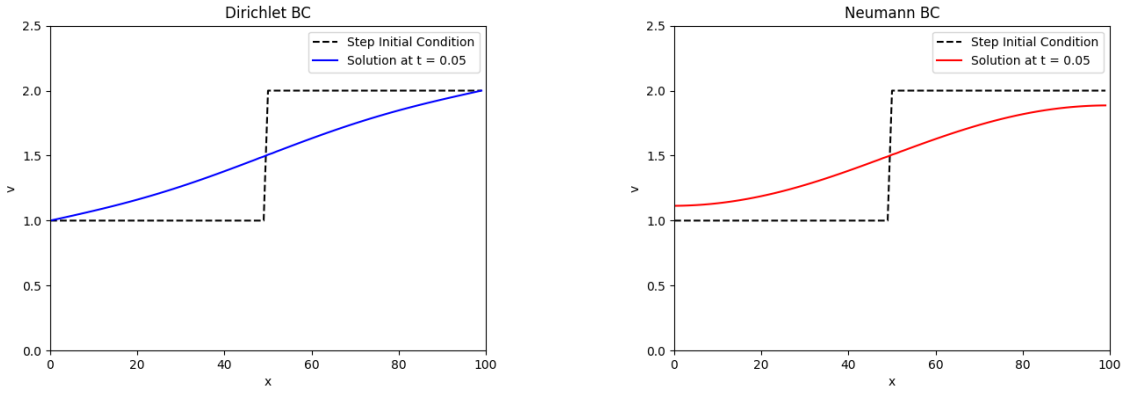

(a) (b)

Figure 1: The solution of a step distribution after evolving for 0.05 seconds in time given fixed (a) and no-flux (b) boundary conditions. At this point, I am using unity for the conductivity, and will correct the time and space scales later.

2α) on the diagonal and $-\alpha$ on the offset diagonals, and $\mathbf{B}$ has $(1-2\alpha)$ on the diagonal and α on the offset diagonals. To solve this matrix equation, the `thomas_method` implements the Thomas Algorithm of Gaussian elimination and backsubstitution, as described in chapter 5 of *Computational Physics*[5].

The results of the simulation so far demonstrate the expected behavior for diffusion given the simple dynamics of the heat equation. As shown in Figure 1, the solver demonstrates the gradual smoothing of the potential profile under both fixed and no-flux boundary conditions.

2.2 Initial Conditions

To allow the user to choose an initial condition for the potential, `initialize_v` offers a selection of preset distributions. The `'uniform'` condition is the default, and there are options for a `'random'` and a `'step'` distribution. The `'step'` distribution comes close to imitating a voltage shock, which will be a critical case to study when implementing the model to explore the effects of heterogeneous conductivity in the context of defibrillation.

2.3 Boundary Conditions

In the Crank-Nicolson method, the boundary conditions are imposed in the matrices $\mathbf{A}$ and $\mathbf{B}$. I have written initializations for two types of boundary condition so far, and will add others as needed. The first is a Dirichlet boundary condition, which I used first for its simplicity while developing the algorithm. The second condition is a Neumann boundary, or "no-flux" boundary condition, which realistically represents the boundary when simulating an isolated piece of tissue.

2.4 Heterogeneous Conductivity

In the `cn_init_1D` routine, I have built in an option to create a heterogeneous conductivity profile. At present, I have used a naïve approach of simply changing the conductivity pointwise when calculating the **A** and **B** matrices. I will need to revisit this analytically to check the validity of this method.

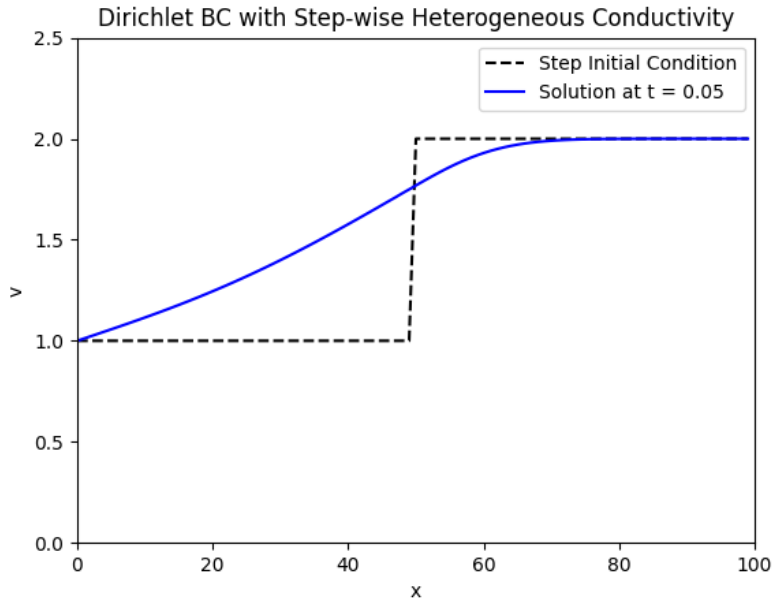

Figure 2: In this simulation, the conductivity of the right half of the domain is 10% of the conductivity of the left half.

3 Next Steps

There is still much to build in order to realize the full bidomain model. The main challenge that I have encountered is that this is a very involved problem with many moving parts, and my approach so far has been to create modular solutions to each step of the problem. What I currently have is effectively a "monodomain" model with no coupling between the external and internal potential. The next steps are as follows:

- Introduce V_e and write a routine to evolve the second equation of the bidomain model, which is time independent. I will be cannibalizing this from past homeworks, so this will be fast.
- Build an IonModel class based on the simplified Hodgkin Huxley model of ion currents.
- Use my modules that initialize the boundaries and heterogeneous conductivity to simulate the full model under conditions mimicking defibrillation

Fortunately, the next steps build on the framework that I have established, with the complex parts mostly modifying the matrix initialization module. Future challenges include formulating the full model efficiently in a way that allows parallelization if time permits. The final step, running the simulation for physiologically interesting use cases, will require me to define a realistic set of parameters for the cell capactitance and ion channel conductivities, for which I will reference the literature.

4 List of Figures

1. Time Evolution of Transmembrane Potential, with the potential plotted at selected time intervals as a function of position.
2. Conduction Velocity vs. Conductance and Surface-to-Volume ratio, plotted as a heat map.
3. Action Potential plot showing the shape of the potential wavefront passing through a single grid point over time.
4. Current vs. Time plots showing the ion currents corresponding to each channel term.
5. Plot of the spatial variance of the potential for varying configurations of heterogeneous conductivity.

References

[1] Peter S. Rabinovitch and J. Paul Robinson. Overview of functional cell assays. *Current Protocols in Cytometry*, Chapter 9:Unit 9.1, May 2002.

[2] Yoram Rudy and Jonathan R. Silva. Computational biology in the study of cardiac ion channels and cell electrophysiology. *Quarterly reviews of biophysics*, 39(1):57–116, February 2006.

[3] Natalia Trayanova, Kirill Skouibine, and Felipe Aguel. The role of cardiac tissue structure in defibrillation. *Chaos (Woodbury, N.Y.)*, 8(1):221–233, March 1998.

[4] Adam Connolly, Edward Vigmond, and Martin Bishop. Virtual electrodes around anatomical structures and their roles in defibrillation. *PLoS ONE*, 12(3):e0173324, March 2017.

[5] M. E. J. (Mark E. J.) Newman. *Computational physics*. [Createspace], Place of publication not identified, 2012.

[6] Robert Plonsey. Bioelectric sources arising in excitable fibers (alza lecture). *Annals of Biomedical Engineering*, 16(6):519–546, November 1988.

[7] Yanyan Claire Ji and Flavio H. Fenton. Numerical solutions of reaction-diffusion equations: Application to neural and cardiac models. *American Journal of Physics*, 84(8):626–638, 08 2016.